

COMPARISON BETWEEN EXPERIMENTAL AND SIMULATION RESULTS OF ROTOR-BEARING SYSTEM CONSIDERING FLUID-INDUCED INSTABILITIES

Hélio Fiori de Castro

State University of Campinas – Mechanical Engineering Faculty – Department of Mechanical Design
Rua Mendeleiev, s/n - Cidade Universitária "Zeferino Vaz" Barão Geraldo - Campinas - SP
heliofc@fem.unicamp.br

Katia Lucchesi Cavalca

State University of Campinas – Mechanical Engineering Faculty – Department of Mechanical Design
Rua Mendeleiev, s/n - Cidade Universitária "Zeferino Vaz" Barão Geraldo - Campinas - SP
katia@fem.unicamp.br

Abstract. *Linear models and synchronous response are generally adequate to describe and analyze rotors supported by hydrodynamic bearings. Hence, stiffness and damping coefficients can provide a good model for a considerable range of situations. However, there are some cases where this model is not sufficient to describe some dynamic phenomenon. Besides, unstable motion occurs, due to precessional orbits at the rotor-bearing-system. This fluid-induced instability is called "oil whirl" or "oil whip". The oil whirl instability occurs in a subsynchronous motion at about one-half of the running speed, and it remains until the speed of the rotor reaches twice the natural frequency of the system. The oil whip is a subsynchronous motion at the natural frequency of the system and it starts at a rotational speed of twice the natural frequency. A flexible rotor with a central disc is modeled and unbalance excitation is assumed. In order to describe the dynamic behavior of the bearing, this work considers a non-linear hydrodynamic bearing model. It is assumed short bearing and laminar flow. The variation of the rotational speed is also taken into account, so that the instability effect can be observed in the simulation results. Experimental results are obtained to compare with the simulations*

Keywords: *hydrodynamic journal bearings, fluid-induced instability, non-linear model*

1. INTRODUCTION

The rotordynamic analysis is becoming a previous phase of study to the design, due to the possibility of predicting problems during the operation of the system. So, mathematical models were developed, in order to represent real machines with considerable confidence. So, several researches were pointed to determine better models to rotating machinery as turbogenerators and multi stage pumps, which are horizontal rotating machines of high load capacity. Some of these numeric simulations were developed to study cylindrical hydrodynamic bearings by Capone (1986 and 1991), where the orbits of the shaft in the bearings can be obtained, considering a non-linear hydrodynamic force model.

The interaction between the rotating system and the oil film in a hydrodynamic bearing causes unstable dynamic behavior (see Gash et al., 2002), which is characterized by a sub-synchronous forward precessional vibration. This dynamic behavior can be called oil whirl and oil whip, which was discovered by Newkirk (1924, 1925), and recently analyzed by Muszynska (1986 and 1988), Crandall (1990), Childs (1993) and Castro et al. (2006).

These fluid-induced instabilities are known as self-exciting vibration of a rotor-bearing system. The oil whirl vibrates in a frequency close to half of the rotation speed. When the rotation speed reaches twice the first natural frequency, the oil whip instability, which can be severally harmful for the rotor-bearing system, starts to act. In this case, the vibration frequency (or self-excitation frequency) is equal to the first natural frequency.

These two manifestations of fluid-induced instability can be associated to the bearing stiffness and the shaft stiffness. If the journal is close to the bearing center, the bearing stiffness is much lower than the shaft stiffness. In that case, the system stiffness is mainly controlled by the bearing stiffness and the fluid-induced instability occurs by the oil whirl, see Muszynska and Bently (1989) and Bently (2001).

Castro et al. (2006) considered a hydrodynamic journal bearing non-linear model, see Capone (1986 and 1991) to simulated fluid-induced instabilities (oil whirl and oil whip), verifying that this model is able to represent numerically the dynamic behavior of rotor under fluid-induced instabilities in transient motion, so that it is possible to make an instability analysis, according to Muszynska (1986 and 1988), Crandall (1990) and Childs (1993). The influence of unbalance was carried out and is in accordance with Muszynska results (1986 and 1988).

The present paper proposes a comparison between the model used by Castro et al. (2006) and experimental results obtained from a horizontal test-rig, where tests with different bearing radial clearance and oil temperature were carried out for this comparison.

2. MATHEMATICAL MODEL

The mathematical model (adopted in this work) of a rotating system can be divided in two parts; the finite element model of the shaft and the concentrated mass to the disk (see Archer, 1965, Ruhl and Booker, 1972 and Nelson and McVaugh, 1976), and the non-linear hydrodynamic supporting forces (Capone, 1986 and 1991) of the cylindrical journal bearing, which is obtained by the Reynolds' equation solution for short bearings.

Equation (1) describes the pressure distribution inside the cylindrical journal bearing (Fig. 1.a), based on the Reynolds' equation (Reynolds, 1886) solution for laminar flux condition. This expression considers the nondimensional oil thickness h and the axial gradient z , due to the losses of lubricating fluid in short journal bearing.

$$\frac{\partial}{\partial v} \left(h^3 \cdot \frac{\partial p}{\partial v} \right) + k^2 \cdot \frac{\partial}{\partial z} \left(\frac{h^3}{\mu} \cdot \frac{\partial p}{\partial z} \right) = \frac{\partial h}{\partial v} + 2 \cdot \frac{dh}{d\tau} \quad (1)$$

The pressure gradient in circumferential direction can be neglected for short journal bearing in relation to the axial gradient (Childs, 1993). Therefore, the result of the differential equation with this simplification is:

$$p(v, z) = \frac{1}{2} \left(\frac{L}{D} \right)^2 \left[\frac{(x - 2\dot{y}) \cdot \sin(v) - (y + 2\dot{x}) \cdot \cos(v)}{(1 - x \cdot \cos(v) - y \cdot \sin(v))^3} \right] \cdot (4 \cdot z^2 - 1) \quad (2)$$

In order to determine the force generated by the oil film pressure distribution, the shaft contact area, $dA = R \cdot dv \cdot L \cdot dz$, is considered in Eq. (3):

$$Fh = \begin{Bmatrix} Fh_x \\ Fh_y \end{Bmatrix} = -\mu \dot{\varphi} \left(\frac{R^2}{C^2} \right) \left(\frac{L^2}{D^2} \right) (R \cdot L) \frac{[(x - 2\dot{y})^2 + (y + 2\dot{x})^2]^{\frac{1}{2}}}{(1 - x^2 - y^2)} \begin{Bmatrix} 3xV(x, y, \alpha) - \sin(\alpha)G(x, y, \alpha) - 2\cos(\alpha)F(x, y, \alpha) \\ 3yV(x, y, \alpha) - \cos(\alpha)G(x, y, \alpha) - 2\sin(\alpha)F(x, y, \alpha) \end{Bmatrix} \quad (3)$$

Where the terms V , G , F and α are respectively given in Eq. (4), (5), (6) and (7), the bearing parameters are radial clearance C , bearing length L , bearing radius R and oil viscosity μ and the rotation speed is $\dot{\varphi}$.

$$V(x, y, \alpha) = \frac{2 + (y \cdot \cos(\alpha) - x \cdot \sin(\alpha)) \cdot G(x, y, \alpha)}{(1 - x^2 - y^2)} \quad (4)$$

$$G(x, y, \alpha) = \int_{\alpha}^{\alpha+\pi} \frac{dv}{(1 - x \cdot \cos(v) - y \cdot \sin(v))} = \frac{\pi}{\sqrt{1 - x^2 - y^2}} - \frac{2}{\sqrt{1 - x^2 - y^2}} \cdot \arctg \left(\frac{y \cdot \cos(\alpha) - x \cdot \sin(\alpha)}{\sqrt{1 - x^2 - y^2}} \right) \quad (5)$$

$$F(x, y, \alpha) = \frac{(x \cdot \cos(\alpha) + y \cdot \sin(\alpha))}{(1 - x^2 - y^2)} \quad (6)$$

$$\alpha = \tan^{-1} \left(\frac{y + 2\dot{x}}{x - 2\dot{y}} \right) - \frac{\pi}{2} \cdot \text{sign} \left(\frac{y + 2\dot{x}}{x - 2\dot{y}} \right) - \frac{\pi}{2} \cdot \text{sign}(y + 2\dot{x}) \quad (7)$$

The differential equation of motion has to be written in two coordinates, x and y , respectively Eq. (8) and (9). To consider the rotating system angular acceleration $\ddot{\varphi}$ as proposed, Eq. (10) relates the input torque of the motor with the rotation of the system. This equation was obtained by Lagrange equation and considered the coupling between torsional and lateral vibration. Meanwhile, this couple is weak and can be neglected, see Childs (1993). Then, Eq. (10) is reduced to Eq. (11).

$$[M] \cdot \ddot{x} + [C] \cdot \dot{x} + [K] \cdot x = Fh_x(x, y, \dot{x}, \dot{y}) + m \cdot e \cdot (\ddot{\varphi} \cdot \sin \varphi + \dot{\varphi}^2 \cos \varphi) \quad (8)$$

$$[M] \cdot \ddot{y} + [C] \cdot \dot{y} + [K] \cdot y = Fh_y(x, y, \dot{x}, \dot{y}) + m \cdot e \cdot (\dot{\varphi}^2 \sin \varphi - \ddot{\varphi} \cdot \cos \varphi) - W \quad (9)$$

$$J_z \cdot \ddot{\phi} \equiv T_Z + m \cdot e \cdot (\sin \phi \cdot \ddot{x} - \cos \phi \cdot \ddot{y} + \dot{\phi} \cdot \dot{x} \cdot \cos \phi + \dot{\phi} \cdot \dot{y} \cdot \sin \phi) \quad (10)$$

$$J_z \cdot \ddot{\phi} \equiv T_Z \quad (11)$$

In order to determine the mass and stiffness matrices $[M]$ and $[K]$, a finite element method is used, to the shaft and the concentrated mass of the rotor.

The shaft damping matrix $[C]$ contains one part which is proportional to the stiffness matrix, and the gyroscopic effects ($[C] = \beta \cdot [K] + \dot{\phi} [G]$). The gyroscopic matrix is also obtained by a finite element method.

The solution of the equation of motion is obtained by numerical methods. In that case, the Newmark integration method was chosen, because it is a robust algorithm to solve non-linear equations in time domain.

In order to proceed with the simulations, a finite element model is considered. Figure 1 represents the horizontal rotor (Fig. 1.b) and its finite element model (Fig. 1.c).

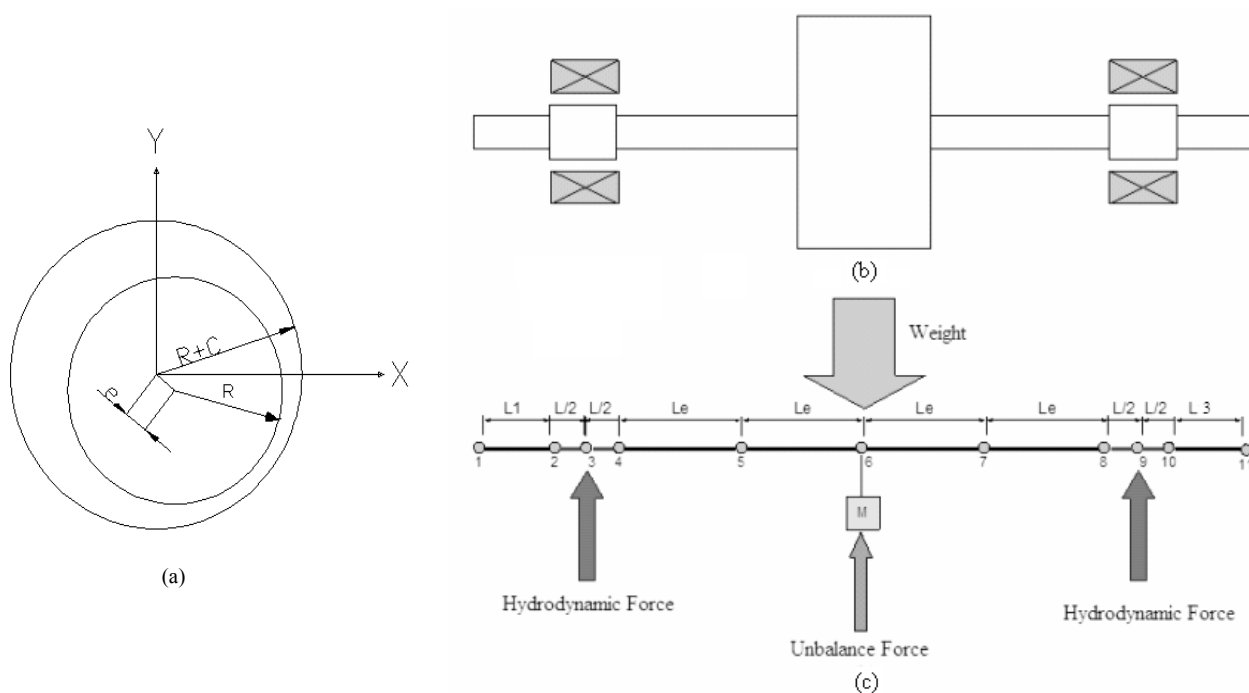


Figure 1. (a) (b) Horizontal Rotor physical model; (c) Horizontal Rotor Finite Element Model.

3. EXPERIMENTAL TEST-RIG

The experimental set up consists in two hydrodynamic bearings and one unbalanced mass assembled in the shaft middle (Fig. 2), as the rotor model shown in Fig. 1. The total length between the bearings is 600 mm. The shaft diameter is 12 mm. The concentrated mass consists of a disk of external diameter of 95 mm and length of 47 mm with mass of 2.3 kg.

A pair of cylindrical hydrodynamic bearings is used to support the shaft, which is in brass, with two different radial clearances of 90 and 125 μm , bearing radius of 31 mm and bearing length of 20 mm. The bearings lubrication uses oil AWS 32.

The acquisition of time response to unbalance was made in the concentrated mass of the rotor. In order to obtain the curves in the horizontal and vertical directions, two magnetic proximity sensors monitor the orbit of the rotor mass.

To monitor the displacement of the shaft inside the bearings, two magnetic proximity sensors are used immersed in the oil film. Thermocouples are also assembled to measure the oil temperature and force transducers to measure the bearing supporting forces in horizontal and vertical directions. The sensors installed in the bearing are shown in Fig. 3.

A temperature controller system controls the oil temperature in the bearing

Three configurations, given in Tab. 1, were carried out to the experimental tests, changing the oil temperature, and consequently the oil viscosity, and bearing radial clearance. The unbalance moment were determined by the method proposed and tested by Castro and Cavalca (2006).

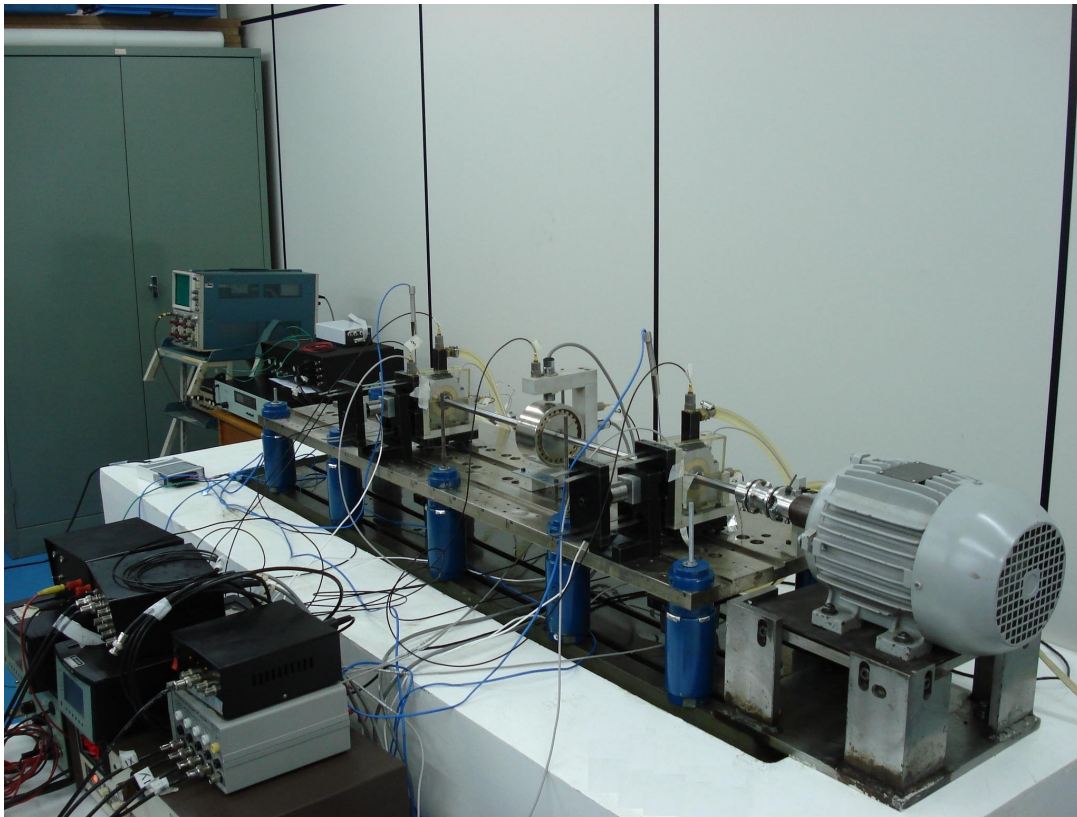


Figure 2. Experimental Set-up.

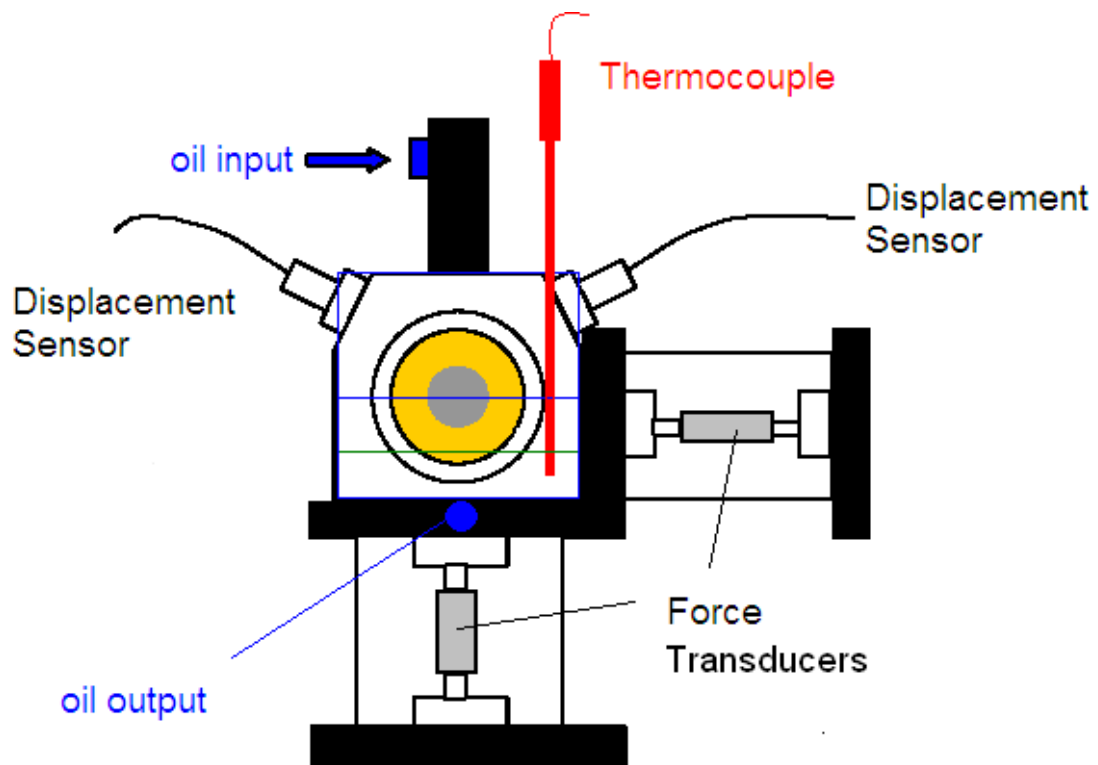


Figure 3. Instrumentation in the bearings.

Table 1. Experimental configurations

Configuration	Oil temperature (°C)	Bearing Radial Clearance (µm)	slenderness ratios (L/D)	Unbalance Moment (kg-m)
1	35	90	0.64	0.0002
2	25	90	0.64	0.0002
3	35	125	0.64	0.0001

As the displacement magnitude can be very high and, consequently, very harmful to the rotating system, a run-down test is carried out. Figure 4 shows the variation of the speed rotation in time domain for the test. Firstly, a fast run-up is carried on, followed by a slow run-down.

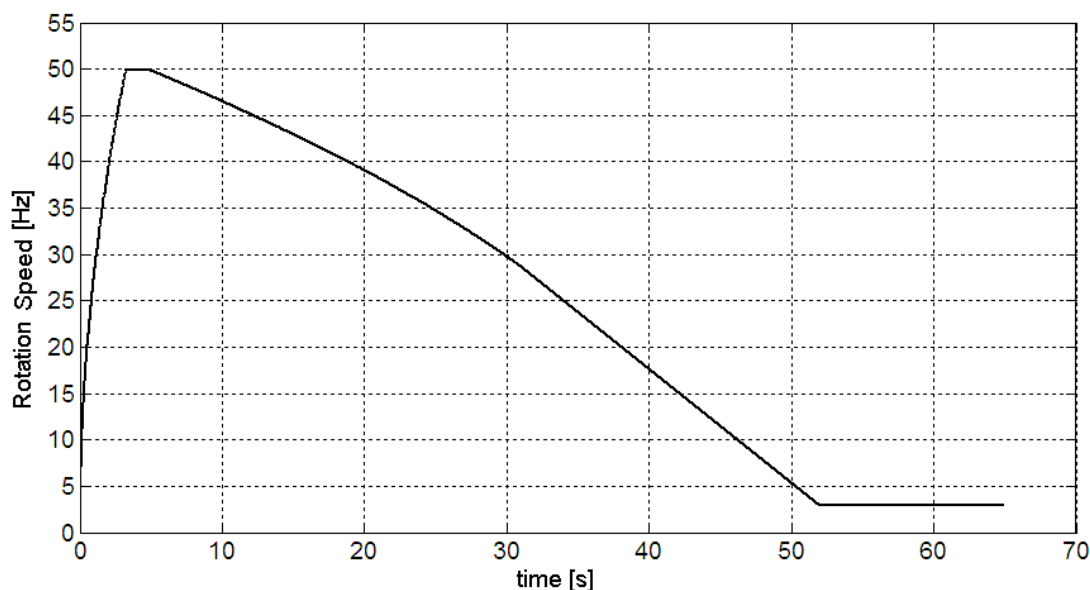


Figure 4. Variation of the rotation speed in time domain for run-down test.

The displacements in the mass for configuration 1 are shown in Fig. 5. The first significant magnitude increasing at 22 Hz is due to the resonance speed of the rotor and the second is due to the fluid-induced instability.

4. COMPARISON BETWEEN SIMULATIONS AND EXPERIMENTAL RESULTS

In order to compare the simulations of the model proposed in section 2 and the experimental results, the displacements of bearing 1 were considered. Figure 6 shows a waterfall plot of the experimental displacements in bearing 1 for the first configuration.

The experimental results also present vibrations in the second and third harmonic, as it can be seen in Fig. 6. The fluid-induced instability is characterized only by the oil whip phenomenon, which starts when the rotation speed is close to twice the resonance speed and the excitation frequency is equal to the first natural frequency.

Taking into account the unbalance moment of the experimental test-rig, determined by the method proposed by Castro and Cavalca (2006), and the bearings parameters for this configuration, which are shown in Tab. 1, the rotating system was simulated. The simulations results in bearing 1 for the first configuration are presented in Fig. 7.

The simulation results only present the sub-synchronous and synchronous (first harmonic) vibrations. Other effects that can excite other harmonics, as misalignment, are not considered in the model.

The amplitude in the resonance speed is much higher in the simulated results. However, the vibration amplitudes due to the fluid-induced instability are very close. The fluid-induced, starts in both cases, starts when the rotation speed is close to 40 Hz.

It was also considered the experimental results and simulation for configurations 2 and 3. Figures 8 and 9 show the experimental and simulated results respectively in bearing 1 for configuration 2. Analogously, Fig. 10 and 11 presents the results for configuration 3.

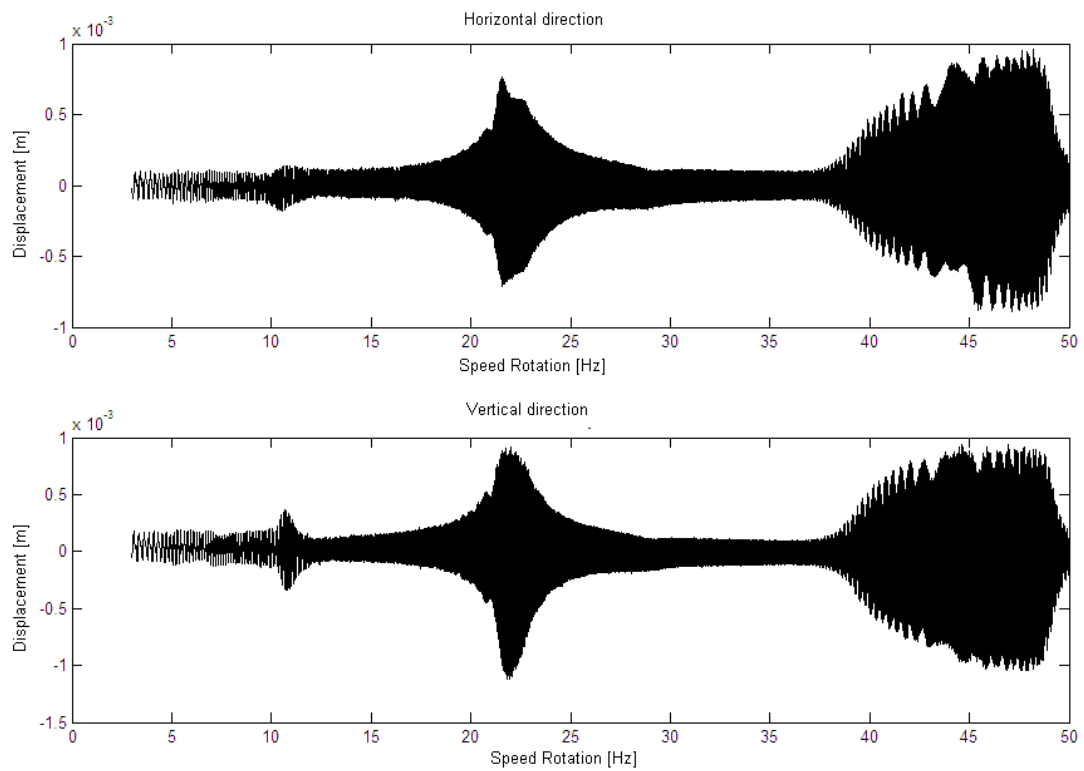


Figure 5. Displacement in the mass for the configuration 1.

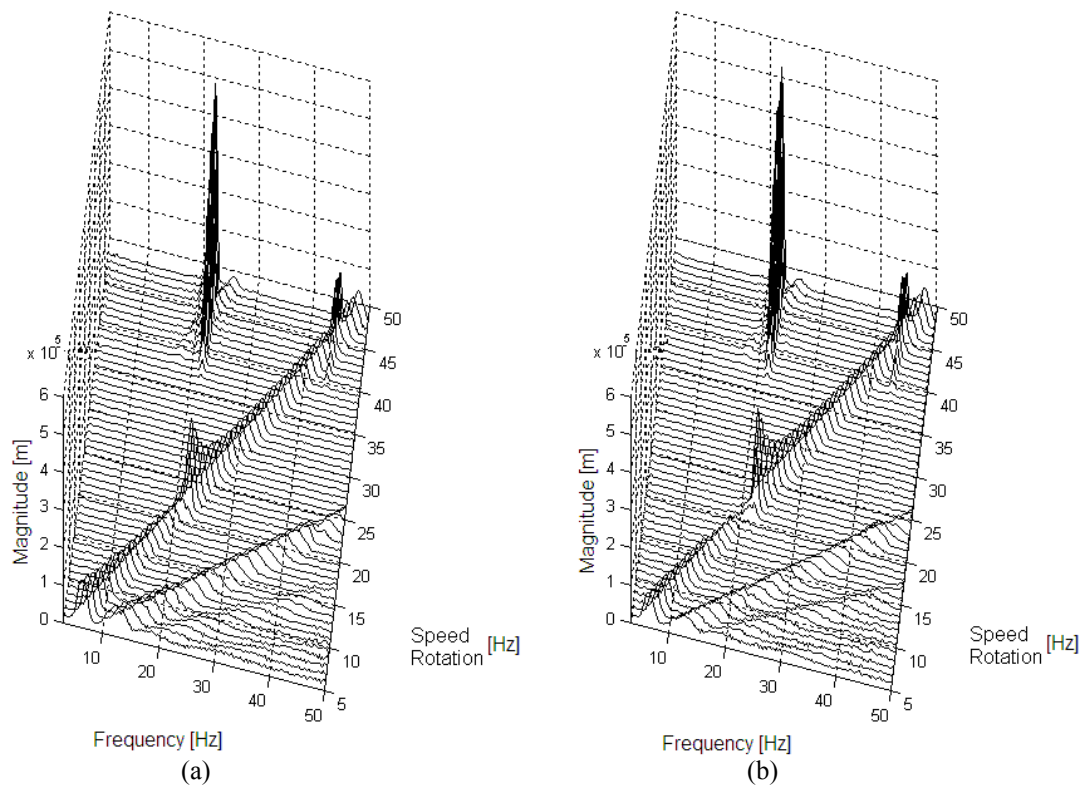


Figure 6. Experimental displacements in bearing 1 for the first configuration: (a) horizontal direction; (b) vertical direction.

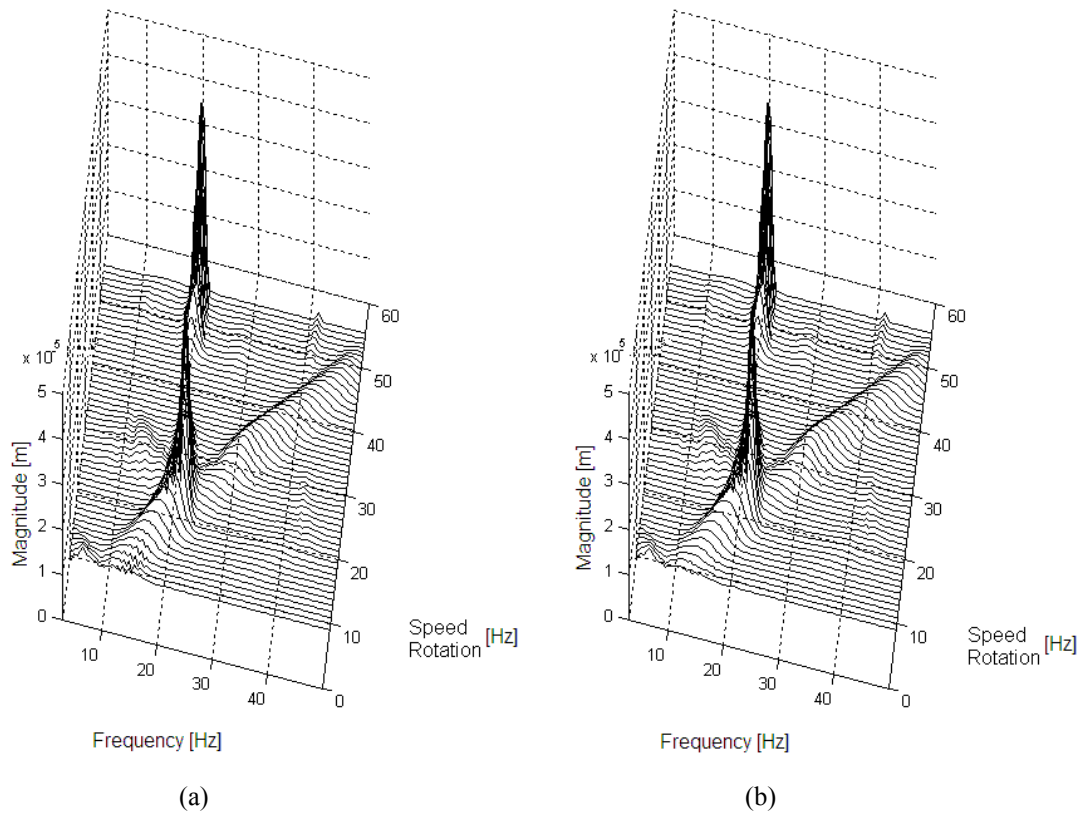


Figure 7. Simulated displacements in bearing 1 for the first configuration: (a) horizontal direction; (b) vertical direction.

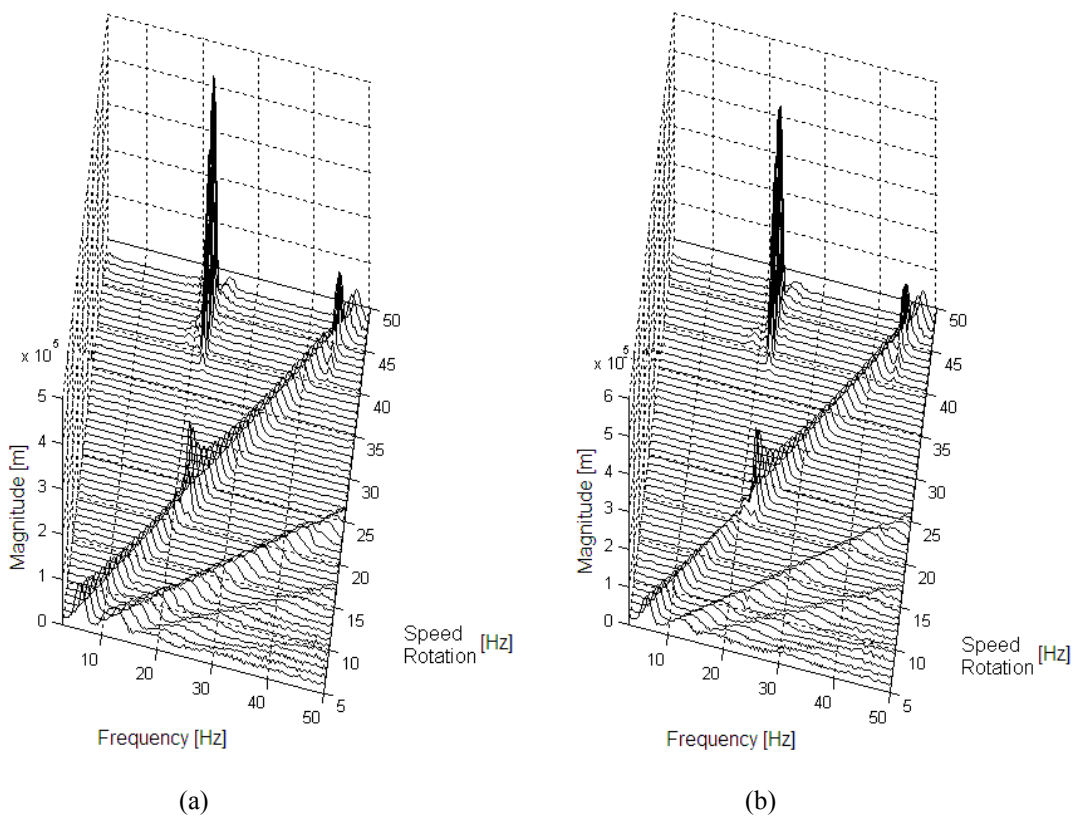


Figure 8. Experimental displacements in bearing 1 for the second configuration: (a) horizontal direction; (b) vertical direction.

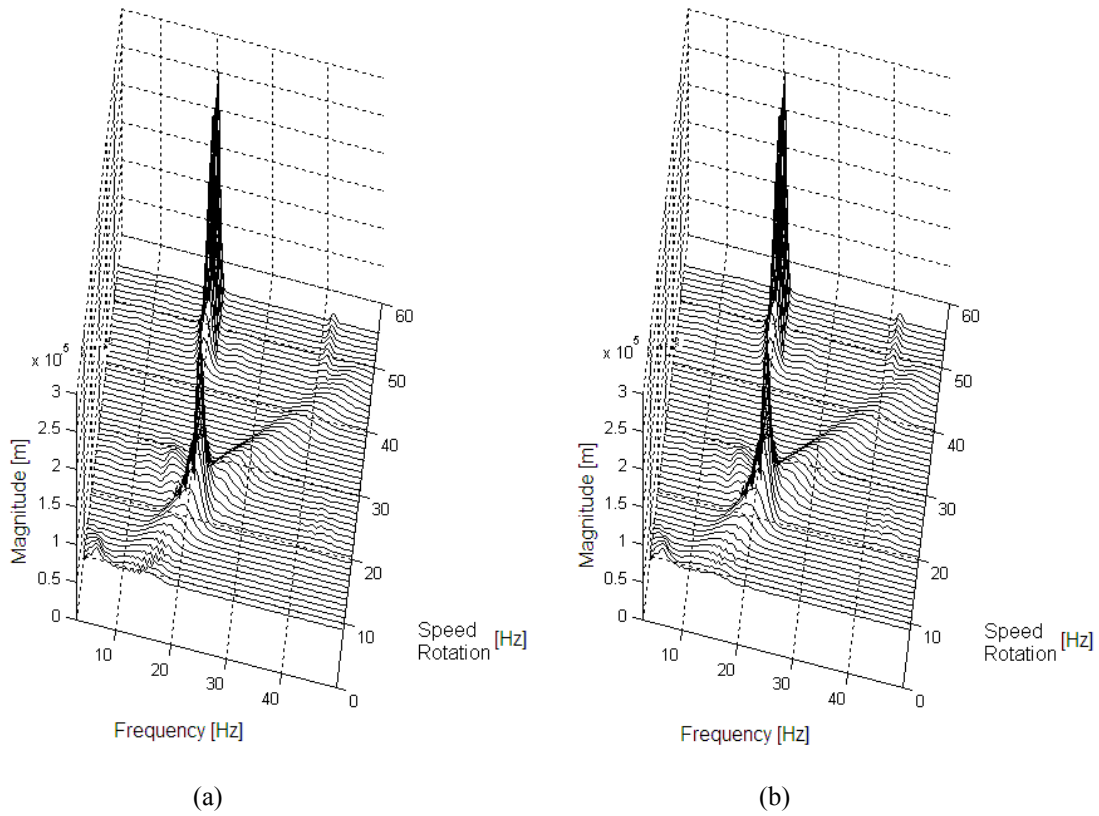


Figure 9. Simulated displacements in bearing 1 for the second configuration: (a) horizontal direction; (b) vertical direction.

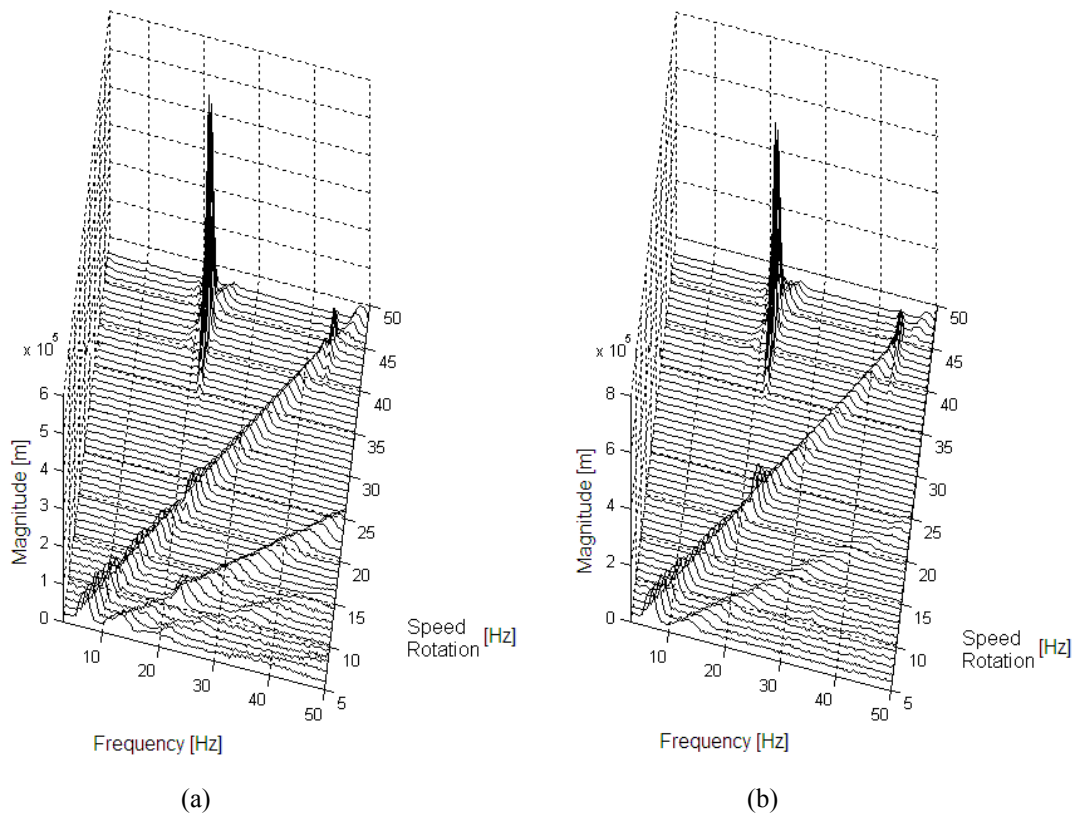


Figure 10. Experimental displacements in bearing 1 for the third configuration: (a) horizontal direction; (b) vertical direction.

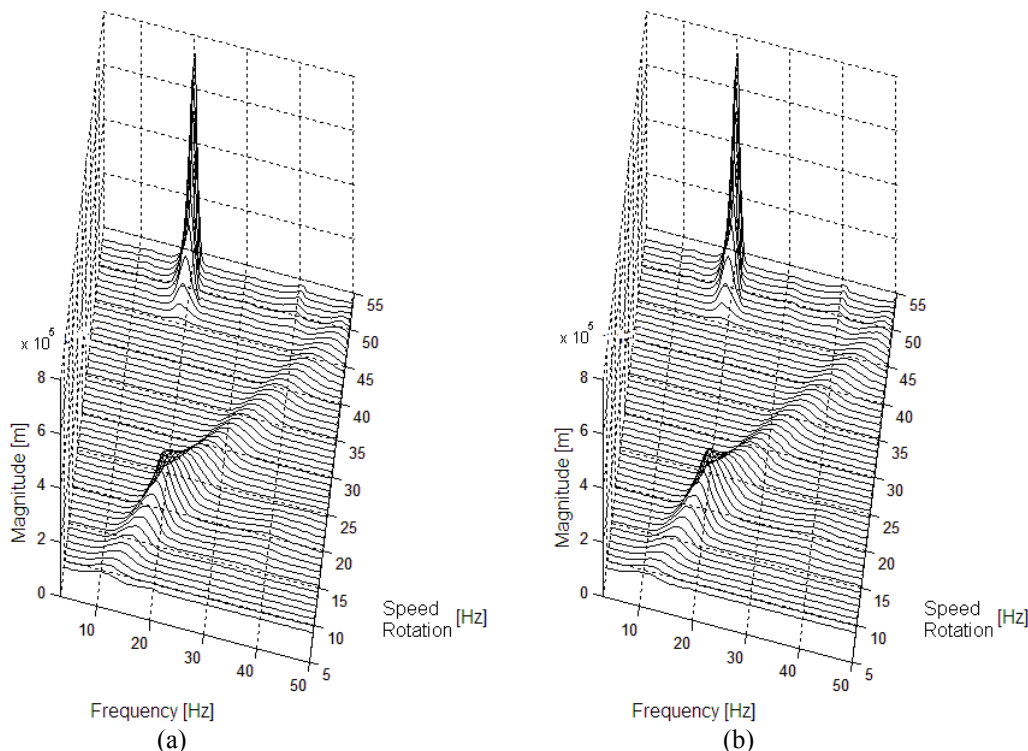


Figure 11. Simulated displacements in bearing 1 for the third configuration: (a) horizontal direction; (b) vertical direction.

The effect of the temperature can be notice by the comparison of configuration 1 and 2. In order to analyze this effect it is necessary to consider Eq. (12), proposed by Ocvirk (1952), which relates the bearing parameters and oil film average pressure p_{avg} . The configuration where the temperature is higher, results in a lower viscosity and consequently in a lower oil pressure. So, the amplitudes are higher in this case. The results in configuration 1 presents higher amplitudes (close to 50 μm in experimental results) than in configuration 2 (close to 45 μm in experimental results), being in accordance with the comments above. The temperature change does not have a significantly influence in the values of the oil-whirl onset speed of instability. In both case the fluid-induced instability starts at approximately 40 Hz. However, a higher difference of temperature should present a significant influence in the oil whirl onset speed of instability.

$$On = \left(\frac{p_{avg}}{\mu \cdot n} \right) \left(\frac{D}{L} \right)^2 \left(\frac{2C}{D} \right)^2 \quad (12)$$

The radial clearance increasing has similar effect in the oil pressure (the oil pressure decrease), see Eq. (12). And this effect can be proved by the comparison between configuration 1 and 3 in the sub-synchronous vibration, where the amplitudes for configuration 3 (close to 60 μm in experimental results) are higher then for configuration 1 (close to 50 μm in experimental results). Otherwise the same effect is not verified in the resonance peak, because of the different identified unbalance moment. This difference does not allow a comparison in the values of the oil-whirl onset speed of instability, because it has a strong influence on this speed (Muszynska, 1986 and 1988).

In all cases the simulations show that the non-linear journal bearing model satisfactory presents the fluid-induced instability effects. However, in many cases it is viable the use of linear models to represents rotating system, but these models are not able to simulate the fluid-induced effect. Muszynska (1986 and 1988) proposed a linear model of bearing forces that was used in a stability analysis, but this model was not applied in simulations to reproduce the displacements of a rotating system as the Capone (1986 and 1991) non-linear model applied in the present work.

It is important to highlight that there are expressive supersynchronous components on the rotor response, which are not shown on the computational results, because the adopted model does not consider some dynamic effects as misalignment.

The expressive peak on the computed synchronous response (Figs. 7 and 9), which does not appear on the experimental results, is probably due to the assumption of a lower proportional structural damping coefficient β , because this parameter was not estimated from the experimental results.

There is a synchronous vibration between 45 and 50 Hz in the experimental results due to the support structure natural frequency

5. CONCLUSIONS

A model of rotor-bearing system is proposed, considering non-linear hydrodynamics forces. The shaft and disk of the rotor are modeled by finite element model. Horizontal rotor was simulated. The influence of hydrodynamic journal bearing parameters like oil film viscosity and radial clearance were analyzed. The proposed model is used in numerical simulations of the rotor run-down to analyze the dynamic behavior of the bearings and compare with experimental results.

The journal bearing non-linear model (Capone, 1986 and 1991) is able to represent oil whirl and oil whip in the numerical simulation, presenting potentiality to reproduce displacements and hydrodynamic journal bearing forces quite well.

The increasing of the oil film viscosity leads to a lower displacement due to the subsynchronous vibration caused by the oil film instability. The same effect can be verified by the decreasing of radial clearance. Finally, these effects can be compared to the Ocvirk number (Ocvirk, 1952), which relate the journal bearing average pressure to the bearing design parameters.

Experimental measurements on the test-rig were carried out with satisfactory results. Therefore, the comparison enables the non-linear hydrodynamic journal bearing model as a viable solution to be applied in rotor-bearing system simulation, when fluid-induced instabilities are considered.

6. ACKNOWLEDGEMENTS

The authors thank CAPES, CNPq and FAPESP for the support to this research.

7. REFERENCES

- Archer, J. S. , 1965, "Consistent Matrix Formulations for Structural Analysis Using Finite-Element Techniques", AIAA Journal, v. 3, n. 10, pp. 1910-1918.
- Bently, R, 2001, "The Death of Whirl and Whip", Bently Nevada Corporation ORBIT, fourth quarter, pp. 42-46.
- Capone, G., 1986, "Orbital motions of rigid symmetric rotor supported on journal bearings", La Meccanica Italiana, n. 199, pp. 37-46.
- Capone, G., 1991, "Descrizione analitica del campo di forze fluidodinamico nei cuscinetti cilindrici lubrificati", L.Energia Elettrica, n. 3, pp. 105-110.
- Castro, H F, Cavalca K L, Nordmann R., 2006, "Rotor-bearing system instabilities considering a non-linear hydrodynamic model", 7th IFToMM - Conference on Rotor Dynamics, Vienna, Austria, paper ID-136, pp. 1-10.
- Castro, H. F., Cavalca, K. L., 2006, "Hybrid meta-heuristic method applied to parameter estimation of a non-linear rotor-bearing system", 7th IFToMM - Conference on Rotor Dynamics. Vienna, Austria, paper ID-135, pp. 1 - 10.
- Childs, D., 1993, Turbomachinery Rotordynamics. Wiley-Intersciences, New York.
- Crandall, S., 1990, "Form Whirl to Whip in Rotordynamics" Transactions of IFToMM 3rd International Conference on Rotordynamics, Lyon, France, pp. 19-26.
- Gasch, R., Nordmann, R., Pfützner, H., 2002, Rotordynamik. Springer, Berlin, 705 p.
- Muszynska, A., 1986, "Whirl and Whip – Rotor Bearing Stability Problems", Journal of Sound and Vibration n. 110 v. 3, pp. 443-462.
- Muszynska, A., 1988, "Stability of Whirl and Whip in Rotor Bearing System", Journal of Sound and Vibration n. 127 v. 1, pp. 49-64.
- Muszynska, A., Bently, D. E., 1989, "Fluid-Generated Instabilities of rotors", Bently Nevada Corporation ORBIT, v. 10, n. 1, pp. 6-14.
- Nelson, H. D., McVaugh, J. M., 1976, "Dynamics of Rotor-Bearing Systems Using Finite Elements", ASME Journal of Engineering for Industry, Vol. 98, pp. 593-600.
- Newkirk, B. L., and Taylor, H. D, 1924, "Shaft Whipping", General Electric Review, Vol. 27, n. 3, 1924, pp. 169-178.
- Newkirk, B. L., and Taylor, H. D., 1925, "Shaft Whipping due to Oil Action in Journal Bearings", General Electric Review, Vol. 28, n. 8, pp. 559-568.
- Ocvirk, E W., 1952, Short bearing approximation for full journal bearings, National Advisory Committee for. Aeronautics, Technical Note 2808, Cornell University.
- Reynolds, O., 1886, "On the Theory of Lubrication and its Application to Mr. Beauchamp Tower's Experiments, including an Experimental Determination of the Viscosity of Olive Oil", Philosophical Transactions of Royal Society of London, Series A, Vol. 177, Part 1, pp.157-234.
- Ruhl, R. L., Booker J. F., 1972, "A Finite Element Model for Distributed Parameter Turborotor Systems", ASME Journal of Engineering for Industry, Vol. 94, p.128-132.

8. RESPONSIBILITY NOTICE

The authors are the only responsible for the printed material included in this paper.